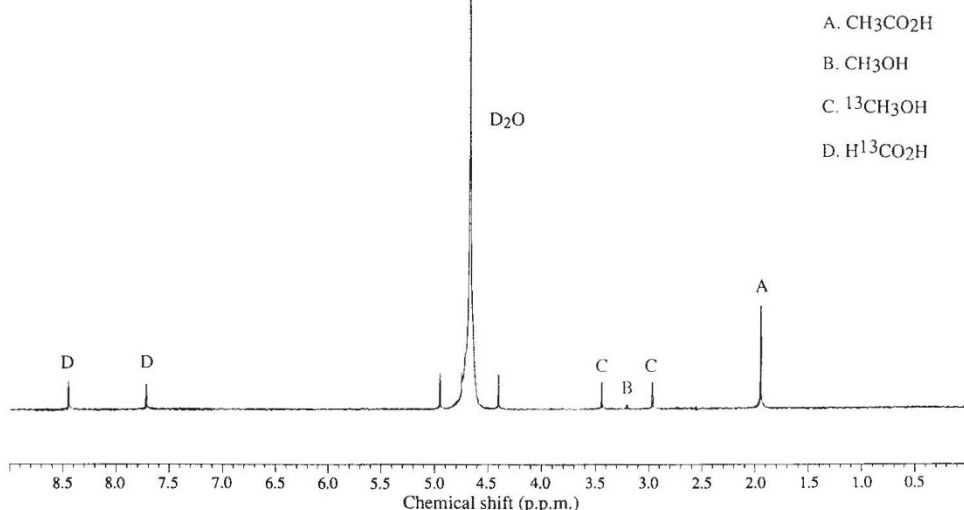


FIG. 2 ^1H -NMR spectrum of the product obtained after reaction between the following compounds at 100 °C for 20 h; RhCl_3 (0.01 M), HI (0.01 M), CH_4 (1,100 p.s.i., 0.06 M in water), $^{13}\text{CH}_3\text{OH}$ (0.06 M), CO (200 p.s.i.), O_2 (50 p.s.i.) and D_2O (5 ml). Chemical shifts with respect to HDO at 4.67 p.p.m.



duct distribution indicated that the hydrolysis rate was substantially slower than the rate of carbonylation to the corresponding $\text{Rh}-\text{C}(\text{O})\text{CH}_3$ species.

Although the functionalization of methane was the focus of our studies, we briefly examined ethane as a substrate. The conversion rate was significantly faster than that observed for methane, but the product specificity was lower. Acetic and propionic acids were formed in similar amounts and, in addition, a significant amount of ethanol was also found. A separate experiment indicated that the acetic acid was derived from ethanol through a subsequent oxidation step. Thus, in contrast to the $\text{Rh}-\text{CH}_3$ species, the rate of hydrolysis of the $\text{Rh}-\text{C}_2\text{H}_5$ intermediate was comparable to the carbonylation rate. These observations find parallels in the fact that the rate of hydrolysis to the corresponding alcohol was substantially faster for $[\text{Cl}_5\text{Pt}-\text{C}_2\text{H}_5]^{2-}$ than for $[\text{Cl}_5\text{Pt}-\text{CH}_3]^{2-}$ (refs 13–15; A. C. Hutson and A.S., unpublished observations).

A key question concerning the present system is the role of the I^- ion as a promoter. As methanol was not carbonylated to acetic acid under our reaction conditions, the function of the added I^- ion cannot be the same as in the Monsanto system⁵. We hope to address this and related mechanistic issues in future studies. □

Received 27 December 1993; accepted 8 March 1994.

1. Masters, C. D., Root, D. H. & Attanasi, E. D. *Science* **253**, 146–152 (1991).
2. Starr, C., Searl, M. F. & Alpert, S. *Science* **256**, 981–987 (1992).
3. Wade, L. E., Gengelbach, R. B., Trumbley, J. L. & Hallbauer, W. L. in *Kirk-Othmer Encyclopedia of Chemical Technology* Vol. 15 298–415 (Wiley, New York, 1981).
4. Wagner, F. S. in *Kirk-Othmer Encyclopedia of Chemical Technology* Vol. 1 124–161 (Wiley, New York, 1978).
5. Forster, D. *Adv. Organomet. Chem.* **17**, 255–267 (1979).
6. Nishiguchi, T., Nakata, K., Takaki, K. & Fujiwara, Y. *Chem. Lett.* 1141–1142 (1992).
7. Lin, M. & Sen, A. J. *Am. chem. Soc., chem. Commun.* 892–893 (1992).
8. *Chem. Engng. News* **71**, July 28, 41 (1993).
9. Lin, M. & Sen, A. J. *Am. chem. Soc.* **114**, 7307–7308 (1992).
10. Whitesides, G. M. et al. *Organometallics* **4**, 1819–1830 (1985).
11. Brown, C., Heaton, B. T., Longhetti, L., Povey, W. T. & Smith, D. O. J. *organomet. Chem.* **192**, 93–99 (1980).
12. Forster, D. *Inorg. Chem.* **8**, 2556–2558 (1969).
13. Sen, A., Lin, M., Kao, L.-C. & Hutson, A. C. J. *Am. chem. Soc.* **114**, 6385–6392 (1992).
14. Luijstra, G. A., Labinger, J. A. & Bercaw, J. E. J. *Am. chem. Soc.* **115**, 3004–3005 (1993).
15. Kusch, L. A., Lavrushko, V. V., Misharin, Yu. S., Moravsky, A. P. & Shilov, A. E. *Nouv. J. Chim.* **7**, 729–733 (1983).

ACKNOWLEDGEMENTS. We thank I. C. Marcovaldo for discussion. This work was funded by the US Gas Research Institute and the US NSF.

Avalanches and power-law behaviour in lung inflation

Béla Sukl*, Albert-László Barabási†,
Zoltán Hantos‡, Ferenc Peták‡
& H. Eugene Stanley†

* Respiratory Research Laboratory,
Department of Biomedical Engineering, Boston University, Boston,
Massachusetts 02215, USA

† Center for Polymer Studies and Department of Physics,
Boston University, Boston, Massachusetts 02215, USA

‡ Departments of Medical Informatics and Experimental Surgery,
Albert Szent-Györgyi Medical University, Szeged, Hungary

WHEN lungs are emptied during exhalation, peripheral airways close up¹. For people with lung disease, they may not reopen for a significant portion of inhalation, impairing gas exchange^{2,3}. A knowledge of the mechanisms that govern reinflation of collapsed regions of lungs is therefore central to the development of ventilation strategies for combating respiratory problems. Here we report measurements of the terminal airway resistance, R_t , during the opening of isolated dog lungs. When inflated by a constant flow, R_t decreases in discrete jumps. We find that the probability distribution of the sizes of the jumps and of the time intervals between them exhibit power-law behaviour over two decades. We develop a model of the inflation process in which ‘avalanches’ of airway openings are seen—with power-law distributions of both the size of avalanches and the time intervals between them—which agree quantitatively with those seen experimentally, and are reminiscent of the power-law behaviour observed for self-organized critical systems⁴. Thus power-law distributions, arising from avalanches associated with threshold phenomena propagating down a branching tree structure, appear to govern the recruitment of terminal airspaces.

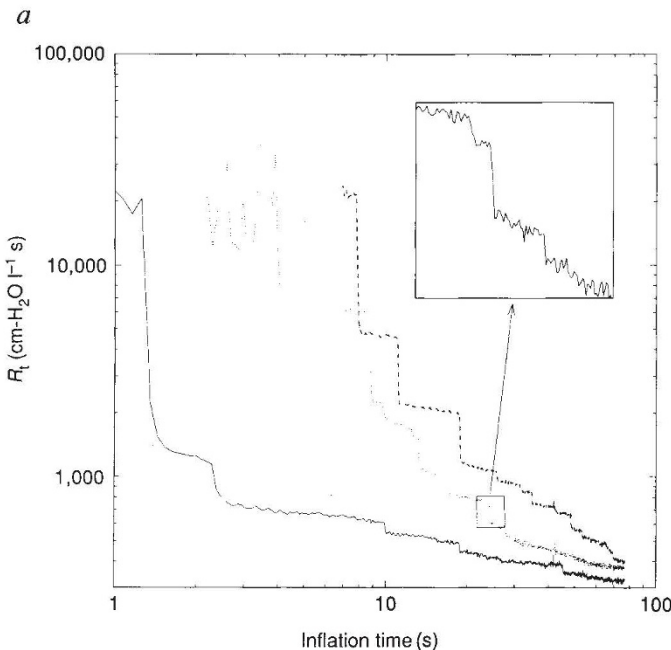
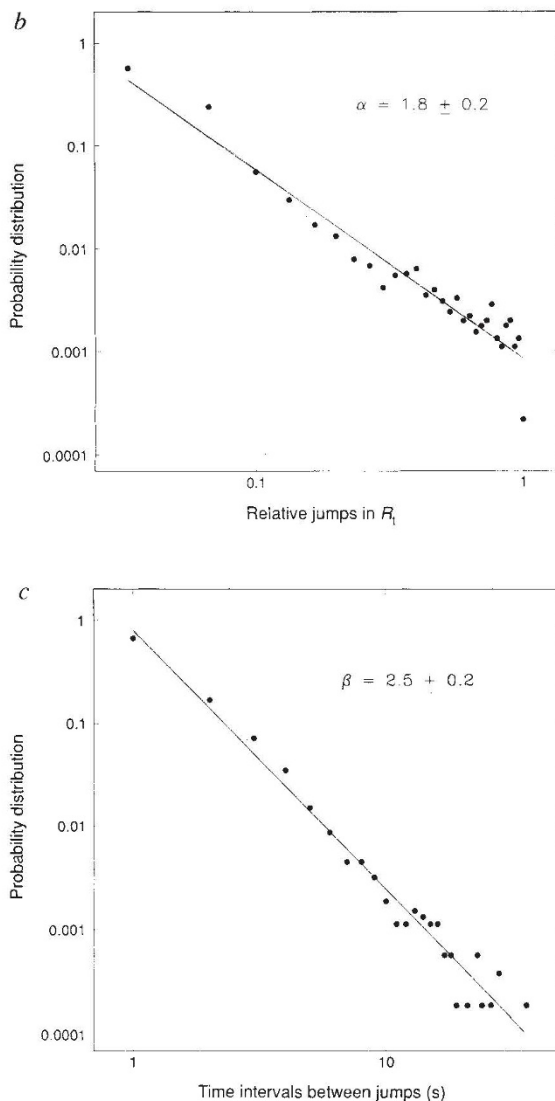


FIG. 1. *a*, The terminal airway resistance R_t as a function of inflation time for three different capsules on a single dog lung lobe. The measurements were carried out using a modification⁶ of the alveolar capsule oscillator technique⁵. Three small plastic capsules were glued to the surface of each isolated dog lung lobe studied. The pleura was punctured, so that the capsules were in communication with the alveolar space through a hole of diameter ~ 0.5 mm. The capsules were connected to a small loudspeaker-in-chamber system through polyethylene catheters. Small amplitude, sinusoidal pressure oscillations with a frequency of 10 Hz were led into the periphery of the lung through the capsules. The input and output pressures of the catheter system were measured with miniature pressure transducers in the loudspeaker chamber, and in a side tap of the capsules, respectively. The local input impedances seen from the capsules were calculated as the load impedance on the catheters. R_t was then obtained as the real part of the local impedance. Note that R_t decreases in discrete jumps as lung volume increases. The magnified portion of the curve (inset) demonstrates the existence of smaller jumps at a smaller scale. The three different line types denote R_t measured in three different capsules *b*, Probability distribution function $\Pi(x)$ of the relative jumps in R_t . We detected the smaller jumps with software that could zoom-in and magnify the desired portions of the curves as shown in *a*. This allowed us to collect from 1,000 to 2,000 discrete jumps from the 10–16 repeated



re-inflations in each lobe from which histograms of the distribution functions were constructed. *c*, Probability distribution function $\Pi(t)$ of the time intervals between jumps in R_t . The straight lines represent the best fits to the data; their slopes give the exponents α and β .

Using the alveolar capsule oscillator technique, R_t was measured during constant-air-flow inflation from residual volume to total lung capacity, TLC, in lung lobes from four dogs^{5,6}. Figure 1*a* shows that during inflation, R_t decreases in well-defined discrete jumps that are superimposed on a continuously decreasing curve. Both the sizes of the jumps and the time intervals between them show a significant variability within a single inflation. When we magnify certain portions of the curves (Fig. 1*a*, inset), we generally find further structures with smaller jumps that are statistically similar to those seen on the entire curves. The magnitudes of the jumps and the time intervals between them vary substantially among capsules. Moreover, these magnitudes and intervals are different even in one capsule when the inflation is repeated.

We quantified the statistical properties of the jumps in R_t by measuring the probability distribution functions $\Pi(x)$ and $\Pi(t)$ of the sizes of the relative jumps x in R_t and the time intervals t between the jumps. Figure 1*b* and *c* demonstrate that the statistics made over the entire data set reveal that both $\Pi(x)$ and $\Pi(t)$ display a range of nearly two decades of their arguments, over which these functions decrease linearly on a

log-log graph. We conclude that $\Pi(x)$ and $\Pi(t)$ follow power-law distributions, that is, $\Pi(x) \approx x^{-\alpha}$ and $\Pi(t) \approx t^{-\beta}$, with $\alpha = 1.8 \pm 0.2$ and $\beta = 2.5 \pm 0.2$. A power-law distribution indicates the lack of a characteristic scale; indeed, it is known that distributions describing phenomena with a characteristic size must decrease exponentially in the ‘wings’, as the wings represent rare events far outside this characteristic size⁷. Thus, our experimental finding of a power-law distribution for the jumps in R_t , and the time intervals between jumps, implies that the opening process is not dominated by any characteristic size scale or characteristic timescale.

uous decrease in R_t . The existence of discontinuities in R_t implies that some fraction of the subtrees joining the primary path open suddenly when the intra-bronchial pressure, P_B , exceeds a threshold value. Indeed, Macklem *et al.* have demonstrated that overcoming a critical (or opening) threshold pressure is necessary to open canine bronchioli⁸, a result supported by a study in flexible-tube models⁹. Furthermore, the time required to open an airway is determined by the viscosity of the fluid film covering the airway wall; this time is well under 0.05 s for the smaller airways⁹. Thus, airways open in such a short time that our measurements detect discontinuous jumps.

To see how the discontinuous jumps in R_t lead to power-law distributions for $\prod(x)$ and $\prod(t)$, we assume that airways do not open independently, but rather in bursts—that is, the opening of one airway may initiate the opening of several more peripheral airways. When P_B exceeds the opening threshold pressure of an airway, all daughter airways in the subtended tree that had a smaller threshold than P_B (or were not closed) would be detected as open. The number of airways, and hence the size of the recruited alveolar volumes involved in such an opening sequence, depends on the size of the subtrees, and can vary substantially. Such a process of sequentially activating different numbers of elements triggered by overcoming a threshold is often termed an avalanche⁴. In complex dynamic systems, the existence of avalanches of very different sizes is thought to lead naturally to power-law dependences^{4,10}.

To test the above interpretation of the observed opening phenomena, we developed a branching-airway model the elements of which are circular elastic tubes of radius r and length l . The airways are assigned a generation number i ($i=0, \dots, N$; N is the order of the tree) and a column number j ($j=0, \dots, 2^i - 1$). The last airways terminate in elastic alveoli represented by equal-sized spheres. An opening threshold pressure P_{ij} is also assigned to each airway (i, j). Opening of an airway occurs when P_{ij} is smaller than the pressure in its parent. Initially, P_{ij} is uniformly distributed between 0 and the value of P_B at TLC; P_B is then increased in small increments. When P_B exceeds P_{00} , the airway (0, 0) opens and its pressure is set equal to P_B . Next, the two airways at $i=1$ are examined to determine whether they can be opened with this value of P_B , that is, if $P_B > P_{10}$ or $P_B > P_{11}$. If one or both conditions are met, then the airways (1, 0) and/or (1, 1) are also opened. This opening process is then continued sequentially down the tree until no airway is found with its $P_{ij} < P_B$. This process thus defines an avalanche in the airways. When the avalanche stops, P_B is incremented and the pressures in all the open airways are updated. We iterate this process until all airways open. The development of such avalanches in a six-generation tree ($2^6 = 64$ alveoli) is illustrated in Fig. 2; in the actual calculations, we use 14 generations ($2^{14} \approx 16,000$ alveoli, 256 times as many).

This model is stochastic in nature: its properties are therefore studied by inflating the lung model for many different realizations of the set of opening threshold pressures P_{ij} in the airways. The R_t as a function of inflation time predicted by our model (Fig. 3a) is remarkably similar to that observed in the experiments (Fig. 1a). Moreover, the statistical properties of R_t that is, the probability distribution functions $\prod(x)$ and $\prod(t)$ (Fig. 3b, c) are also in good agreement with those calculated from the experimental data (Fig. 1b, c). Both functions are power laws, characterized by exponents $\alpha = 1.7 \pm 0.2$ and $\beta = 2.5 \pm 0.2$.

Our model allows us to investigate processes that cannot be measured experimentally. One such process is the recruitment of the newly opened alveolar volumes, v . We calculated the associated probability distribution function, $\prod(v)$, and we find $\prod(v) \approx v^{-\gamma}$, with $\gamma = 1.1 \pm 0.2$. The significance of a power-law distribution is that the probability of finding a large avalanche is much higher than it would be if the distribution were gaussian or exponential. This implies that the newly recruited alveolar volumes following an avalanche can in fact be remarkably large. For example, in the bottom right panel of Fig. 2, the last ava-

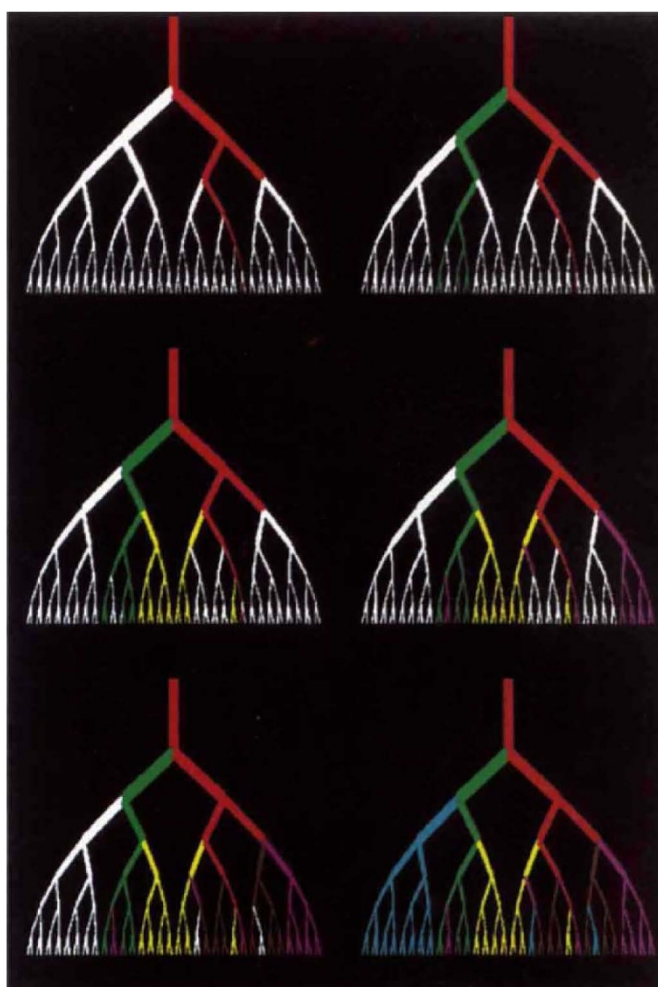


FIG. 2 The development of avalanches in a six-generation airway model. At first (top left), all airways are closed (white) whose threshold values are larger than the intra-bronchial pressure (red), which defines the first avalanche. Then the intra-bronchial pressure increases until a second threshold is exceeded, and as a result all airways further down the tree whose thresholds are smaller become inflated (green). The intra-bronchial pressure is successively increased until a third, fourth, and fifth thresholds are exceeded (yellow, magenta and brown). The last threshold to be exceeded (bottom right) results in filling the airways coloured blue. Note that the alveolar volume opened by an avalanche is proportional to the number of terminal airways that are open. Note also the wide range of avalanche sizes: the first avalanche opens only one terminal airway, whereas in the last avalanche the number of airways opened is more than a factor of ten larger than in the first avalanche, and comprises ~31% of the total number of airways.

che opens up over 30% of the total volume of the model, thereby significantly increasing the total alveolar surface area available for gas exchange. These findings suggest that both the magnitude and timing of pressure excursions applied at the airway entrance during artificial ventilation may be critical in triggering the avalanche process of alveolar recruitment. Furthermore, these processes may also pertain to pathological conditions of the lungs, particularly in the presence of excessive intrabronchial fluid, loss of pulmonary elasticity or increased bronchoconstrictor tone. The establishment of the relationship between the avalanche processes in the airways and various pulmonary function tests awaits further research.

Before concluding, we note that power-law distributions may

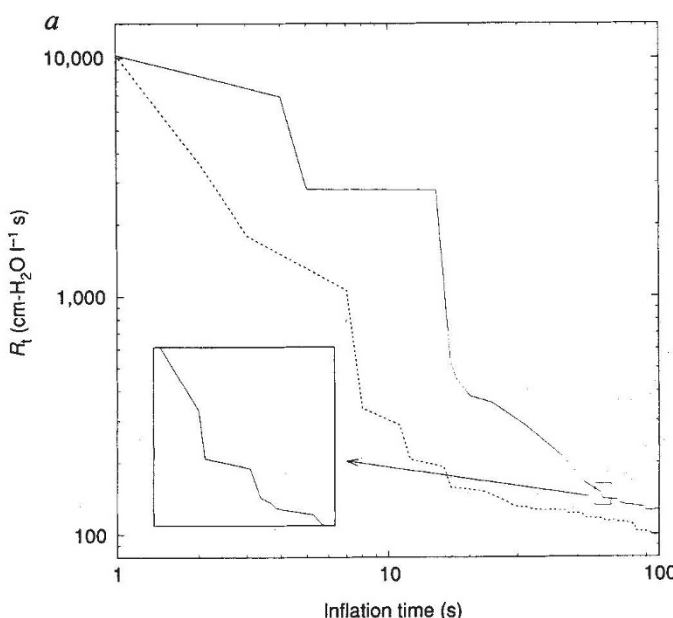
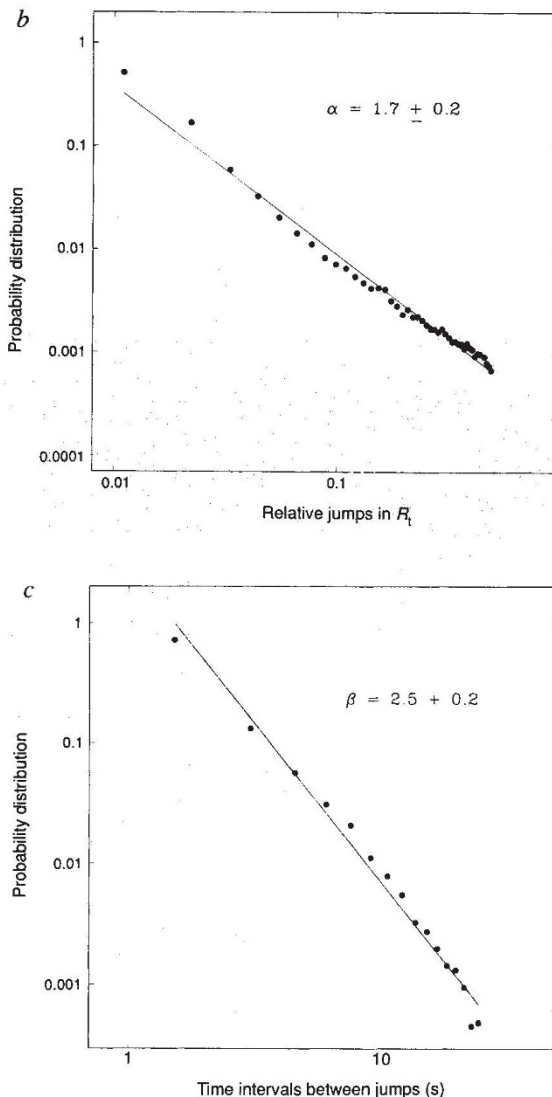


FIG. 3 Prediction of the model for the statistical properties of the terminal airway resistance, calculated for a tree comprising 14 generations. We modelled the peripheral portion of the airway tree, because it is only in these last 14 generations that airway closure was found to occur¹. The dimensions of the airways in the model were assigned by a scaling rule: the radius r_{00} and length l_{00} (see text) were chosen so that they were equal to r and l at the corresponding generation of the morphometric airway data published by Horsfield *et al.*¹⁴. The r and l were made independent of the column index j and were scaled by a factor of 0.86 and 0.9, respectively, from the r and l of the previous generation which are mean values in the Horsfield model¹⁴. Having fixed the dead space of the tree, the size of the alveoli were chosen so that the dead space was 10% of the total alveolar volume which was then uniformly distributed among the terminal airways. The airway walls and the alveolar walls were assumed to be perfectly elastic with their pressure-volume relationships similar to those described by Lambert *et al.*¹⁵ and Salazar and Knowles¹⁶, respectively. At each step of the inflation, the radii of the open branches and the alveoli were updated according to their pressure-volume relationships. Then we calculated R_t of the entire tree, seen from an alveolus, as follows. (1) The complex impedances, at 10 Hz, of all open branches—together with the impedances of the alveoli—were calculated. (2) The total terminal impedance was then obtained by marching up the primary path, starting from the terminal end and adding the next branch or alveolar impedance in the appropriate series or parallel fashion at each node. The real part of this impedance is R_t . **a**, Model-predicted R_t at two alveolar locations as a function of inflation time. Note the similarity between the patterns of



the discrete jumps in the model and those in Fig. 1a. The magnified portion of the curve (inset) demonstrates the existence of smaller jumps at a smaller scale. **b** and **c**, $\Pi(x)$ and $\Pi(t)$, respectively, predicted by the model (dots). The straight lines represent the best fit to the data; their slopes give the exponents α and β . We estimated these probability distribution functions from 2,000 repetitions of the inflation, requiring ~5 h calculation time for an IBM RS-6000 Model 350 work station.

be widespread in biology¹¹: for example, the static distribution of airway radii was reported to follow a power law¹². Until now, dynamic biological processes have not been studied extensively¹³,

but it is possible that the general framework of self-organized criticality⁴ will prove useful for describing a wide range of such phenomena. □

Received 4 January; accepted 18 February 1994.

1. Hughes, J. M. B., Rosenzweig, D. Y. & Kivitz, P. B. *J. appl. Physiol.* **29**, 340–344 (1970).
2. Engel, L. A., Grassino, A. & Anthonisen, N. R. *J. appl. Physiol.* **38**, 1117–1125 (1975).
3. Crawford, A. B. H., Cotton, D. J., Paiva, M. & Engel, L. A. *J. appl. Physiol.* **66**, 2511–2515 (1989).
4. Bak, P., Chen, K. & Creutz, M. *Nature* **342**, 780–783 (1989).
5. Davey, B. L. K. & Bates, J. H. T. *Respir. Physiol.* **93**, 165–182 (1993).
6. Peták, F., Hantos, Z., Adamicza, A., Otis, D. R. & Daróczy, B. *Eur. Respir. J.* **6**, 403S (1993).
7. Vicsek, T. *Fractal Growth Phenomena* 2nd edn (World Scientific, Singapore, 1992).
8. Macklem, P. T., Proctor, D. F. & Hogg, J. C. *Respir. Physiol.* **8**, 191–201 (1970).
9. Gauer, D. P., Samsel, R. W. & Solway J. *J. appl. Physiol.* **69**, 74–85 (1990).
10. Bak, P. & Creutz, M. in *Fractals in Science*. (eds Bunde, A. & Havlin, S.) (Springer, Berlin, 1994).

11. West, B. J. & Shlesinger, M. F. *Am. Scient.* **78**, 40–48 (1990).
12. Shlesinger, M. F. & West, B. J. *Phys. Rev. Lett.* **67**, 2106–2109 (1991).
13. West, B. J. *Fractal Physiology and Chaos in Medicine* (World Scientific, Singapore, 1990).
14. Horsfield, K., Kemp, W. & Phillips, S. J. *appl. Physiol.* **52**, 21–26 (1982).
15. Lambert, R. K., Wilson, T. A., Hyatt, R. E. & Rodart, J. R. *J. appl. Physiol.* **52**, 44–56 (1982).
16. Salazar, E. & Knowles, J. H. *J. appl. Physiol.* **19**, 97–104 (1964).

ACKNOWLEDGEMENTS. We thank R. D. Kamm and J. J. Fredberg for their help in the early stages of this work. We also thank D. R. Otis Jr, A. Adamicza and B. Daróczy for the data collection, and S. V. Buldyrev for comments on the manuscript. This work was supported by an OTKA grant from the Whitaker Foundation, Fogarty IRC award from the US NIH, and grants from the US NIH and NSF.